

CSQF-based Time-Sensitive Flow Scheduling in Long-distance Industrial IoT Networks

Yudong Huang, Tao Huang, *Senior Member, IEEE*, Xinyuan Zhang, Shuo Wang, Hongyang Du, Dusit Niyato, *Fellow, IEEE*, and Fei Richard Yu, *Fellow, IEEE*

Abstract—Booming time-critical services, such as automated manufacturing and remote operations, stipulate increasing demands for facilitating large-scale Industrial Internet of Things (IoT). Recently, a cycle specified queuing and forwarding (CSQF) scheme has been advocated to enhance the Ethernet. However, CSQF only outlines a foundational equipment-level primitive, while how to attain network-wide flow scheduling is not yet determined. Prior endeavors primarily focus on the range of a local area, rendering them unsuitable for long-distance factory interconnection. This paper devises the cycle tags planning (CTP) mechanism, the first integer programming model for the CSQF, which makes the CSQF practical for efficient global flow scheduling. In the CTP model, the per-hop cycle alignment problem is solved by decoupling the long-distance link delay from cyclic queuing time. To avoid queue overflows, we discretize the underlying network resources into cycle-related queue resource blocks and detail the core constraints within multiple periods. Then, two heuristic algorithms named flow offset and cycle shift (FO-CS) and Tabu FO-CS are designed to calculate the flows' cycle tags and maximize the number of schedulable flows, respectively. Evaluation results show that FO-CS increases the number of scheduled flows by 31.2%. The Tabu FO-CS algorithm can schedule 94.45% of flows at the level of 2000 flows.

Index Terms—Bounded Latency, Flow Scheduling, Industrial Internet of Things, Time-Sensitive Networks.

I. INTRODUCTION

The Internet has been prone to congestion, crumble, and long-tail delays in the past few decades. As an emerging branch of the Internet, the Industrial Internet of Things (IoT) is leading a new wave of industrial revolution and network innovation [1] [2]. Different from traditional best-effort transmission of bit information, industrial time-critical applications, such as remote operations [3], smart grid [4], and digital twin [5], require task-oriented delivery with bounded delay and jitter. By leveraging the booming 5G and edge computing technologies, several works [6] [7] have studied the predictable

low-latency communication paradigm within the range of a factory or a local area. However, the possibility of providing long-distance deterministic forwarding services for large-scale cyber-physical systems remains to be explored.

In the sensor-controller-actuator environment of Industrial IoT, many time-sensitive data need to be collected and transmitted to the edge node of the factory or cloud server for further analysis and process. Some of them are aperiodic traffic, such as event alerts and critical message updates, while others exhibit the features of periodic sending. For example, remote control of a slave robotic arm requires issuing kinematic packets every 10 ms to synchronize the Cartesian coordinates, acceleration, and angular velocity information. According to the ITU report [8], machine-type devices could reach 97 billion in 2030. Rapidly growing IoT traffic leaves industrial proprietary buses facing bandwidth shortages, prohibitive costs, and compatibility issues. The Ethernet is on the rise and promises to enable converged industrial networks.

On the one hand, the time-sensitive networking (TSN) is a key candidate to enhance the Ethernet with real-time transmission capability. Since time synchronization struggles with guaranteeing accuracy in large-scale industrial sensor-controller-actuator environments, many TSN scheduling mechanisms, such as time-controlled gating, and cyclic queuing and forwarding (CQF), are limited to layer-2 local area networks (e.g., seven hops advised by the IEEE 802.1D protocol [9]). Moreover, TSN generally assumes that the propagation delay of the link is virtually non-existent, which is infeasible to be directly applied to long-distance networks.

On the other hand, the IETF DetNet working group is currently extending the TSN mechanisms to layer-3 deterministic networks. One of the promising solutions is cycle specified queuing and forwarding (CSQF) [10]. CSQF divides the sending time of an out-port into a series of equal time intervals; each time interval is called a cycle (noted as T). By tagging a sequence of cycle information to the packet headers, packets are expected to be transmitted at precise reserved durations along the path. Hence, once the cycle size and label stacks are determined, the end-to-end latency is bounded. More importantly, the end-to-end jitter is theoretically independent of hop count, which is controlled to no more than $2T$.

CSQF is essentially an underlying primitive that needs the special hardware support [11] for cycle mapping. CENI [12] testbed evaluations have shed light on the performance of devices equipped with CSQF capabilities in real-world systems. However, a cycle tag stack only explicitly defines the cyclic forwarding behavior of a single flow along a linear path.

Y. Huang and X. Zhang are with the State Key Laboratory of Networking and Switching Technology, BUPT, Beijing, 100876, P.R. China (e-mail: hyduni@bupt.edu.cn, zhangxinyuan0181@bupt.edu.cn).

T. Huang and S. Wang are with the State Key Laboratory of Networking and Switching Technology, BUPT, Beijing, 100876, P.R. China. They are also with the Purple Mountain Laboratories, Nanjing, 211111, P.R. China (e-mail: htao@bupt.edu.cn, shuowang@bupt.edu.cn).

H. Du and D. Niyato are with the School of Computer Science and Engineering, Nanyang Technological University, Singapore (e-mail: hongyang001@e.ntu.edu.sg, dniyato@ntu.edu.sg).

F. Richard Yu is with the Department of Systems and Computer Engineering, Carleton University, Ottawa, ON K1S 5B6, Canada (e-mail: richard.yu@carleton.ca).

To make CSQF practical, network administrators necessitate an overarching strategy to effectively orchestrate network-wide traffic. Computing global scheduling cycle tags for time-sensitive flows continues to be a pressing challenge.

The scheduling task is analogous to the bin packing problem, with both being characterized as NP-hard [13] [14]. While numerous TSN flow scheduling schemes [15] [16] have been proposed with the time-controlled gating and CQF, they generally ignore the link delay and cannot reach the goal of long-distance deterministic transmission. Recently, the authors of [14] studied flow scheduling algorithms for CSQF, but their focus was primarily on path generation, utilizing straightforward constraints that only addressed capacity and delay aspects, ignoring the cycle mapping and bounded queue length constraints. Moreover, [14] performs admission control at the flow level, which is incapable of adaptively adjusting the cycle tags, whereas we focus on the per-packet granularity and address the cycle tag computation problem.

It is not trivial to model CSQF. First, in the end-to-end latency calculation, long-distance link delays are hard to normalize and align with cyclic scheduling behaviors, which prevents hop-by-hop delays from being considered a bounded constant value. Second, unlike traditional bandwidth allocation mechanisms, CSQF requires fine-grained time resource allocation. The industrial real-time applications send periodic traffic with different flow sending periods, which further arises challenges to unify cycle-related queue resource model. Third, since multiple flows will compete for the queue resources of each output port along the path, the cycle tag stack needs to be elaborately computed to avoid violating bounded queue length constraints. To our knowledge, this study is the inaugural effort to present the comprehensive integer programming mathematical model for the global scheduling of CSQF.

This paper targets to make the CSQF practical for efficient network-wide flow scheduling in long-distance Industrial IoT networks. The model hypotheses include: (1) Flow features and propagation delays are obtained prior, where flows are a set of periodic unicast flows marked by the highest priority. (2) CSQF-enabled switches adopt frequency synchronization, and the central controller applies zero phase deviation as a general scheduling basis. (3) All industrial terminals can send packets accurately, without considering the jitter from the source node. The main contributions are:

- We present a key insight that queuing delay could be bounded by binding the maximum queue length to a cycle time factor. Then, we establish a novel cycle tags planning (CTP) model¹, where the per-hop cycle alignment problem is solved by decoupling the long-distance link delay from cyclic queuing time. To avoid queue overflows under multi-flow aggregations, we discretize the network resources into cycle-related queue resource blocks and satisfy the bounded queue length requirement by constructing mapping constraints between flow and resource blocks.

- We design a novel heuristic algorithm named flow offset and cycle shift (FO-CS) to incrementally calculate the

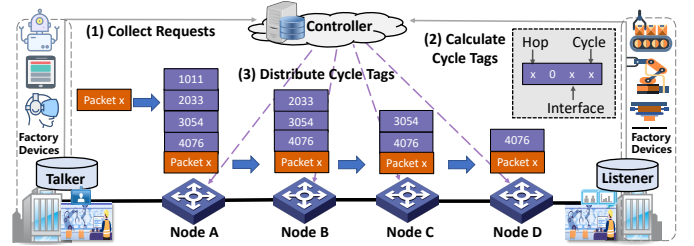


Fig. 1. The working mechanism of CSQF in the factory interconnection or cloud PLC scenarios, where the control plane has to compute the cycle tags (SID labels) for every packet along the path.

network-wide traffic’s cycle tags and quickly generate per-flow scheduling solutions. By leveraging the Tabu search method, we also develop a Tabu FO-CS algorithm to maximize the number of schedulable flows.

- We evaluate the FO-CS algorithm under wide-area topologies in remote industrial control scenarios. Simulation results demonstrate that FO-CS improves the scheduling flow number by 31.2% compared with the naive algorithm. Furthermore, the Tabu FO-CS algorithm can schedule 94.45% of flows at the flow level of 2000 under the realistic topology of Internet2.

The structure of this paper is as follows: Section II provides a brief overview of the CSQF under Industrial IoT scenarios. Section III delves into the motivation. In Section IV, we present the formulation of the CTP model, while Section V details the design of the FO-CS algorithm. Section VI showcases our evaluation results. Related works are discussed in Section VII. The paper concludes in Section VIII.

II. BACKGROUND

Currently, the Industrial IoT has brought a new era of network innovations. Unlike fast-fluctuation TCP applications, in the industrial automation and intelligent manufacturing scenarios, real-time applications (e.g., remote operations and cloud control) issue promised aperiodic/periodic traffic and require the bounded latency of milliseconds and jitter of microseconds [6] [17]. The deterministic networking (DetNet) is generally considered as private WANs, rather than replacing the Internet. The difference is that private WANs allow closed access control while the Internet is managed by large groups of domains. DetNet is compatible with the existing Internet since the best-effort flow can still be transmitted by DetNet.

Table I summarizes the examples of delay, jitter, data rate, and payload size requirements for time-sensitive tasks in typical DetNet scenarios, such as discrete automation, process automation, and electricity distribution, according to 3GPP TS22261 [18] and IETF RFC 8578 [19]. A small payload means it is less than or equal to 256 bytes, and a big payload generally does not exceed the MTU size. Note that all the values in this table are example values, which are varied in specific deployment configurations.

With the efforts of the DetNet working group, a cycle-based scheduling mechanism named CSQF is proposed. In CSQF, the key to achieve predictable latency and bounded jitter lies in the segment routing identifiers (SIDs)². Specifically, each

¹The open-source code of the CTP model is at <https://github.com/Hyduni001/CTP-Model-for-CSQF>.

²The segment routing identifiers (SIDs) are equivalent to the cycle tags.

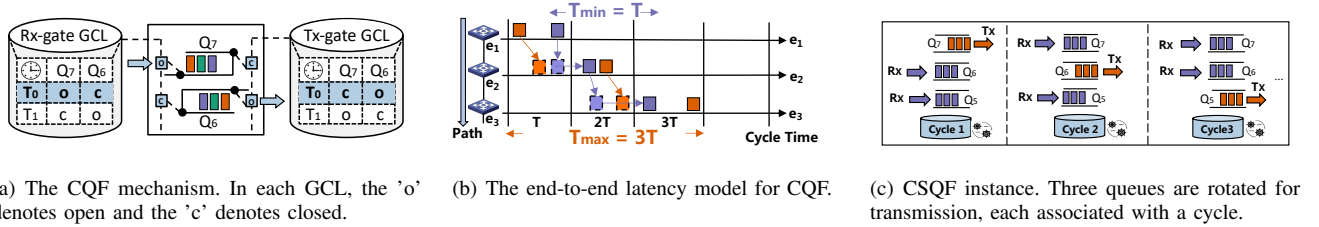


Fig. 2. Comparison of mechanisms evolving from local CQF to CSQF under long-distance Industrial IoT networks.

TABLE I
TYPICAL USECASES AND REQUIREMENTS FOR DETNET

Scenarios / tasks	Latency	Jitter	Data rate	Payload size
Discrete automation	1-10 ms	1-100 μ s	1-10 Mbps	Small to big
Process automation-remote control	50 ms	20 ms	1-100 Mbps	Small to big
Process automation-monitoring	50 ms	20 ms	1 Mbps	Small
Electricity distribution-medium voltage	40-100 ms	1 ms	10 Mbps	Small to big
Electricity distribution-high voltage	5-10 ms	100 μ s	10 Mbps	Small
Electricity distribution-extra-high voltage	5 ms	10 μ s	/	Small
Intelligent transport systems- backhaul	10 ms	20 ms	10 Mbps	Small to big
Tactile interaction	5 ms	TBC	10 Mbps	Small to big

SID is a label recording the packet's output port and sending cycle. For instance, in Fig. 1, the SID of 4076 identifies that the packet x should be sent out from the cycle 6 and the port 7 of the hop 4 (node D). Several SIDs are combined into a label stack that indicates the dedicated forwarding path of the packet. Two data-plane instantiations of segment routing (SR) are SR over MPLS (SR-MPLS) and SR over IPv6 (SRv6). In practice, both SR-MPLS and SRv6 can be used for the SID of CSQF. The label of the sending cycle could be specified in the local segment layer, which is allocated from the Segment Routing Local Block (SRLB) according to RFC8402.

The generation method and workflow of SIDs are as follows: (1) Once a talker at the source intends to issue time-sensitive traffic to a listener at the destination, it uploads the quality of service (QoS) requests to a centralized network controller. (2) The network devices learn from adjacent nodes to establish the cycle mapping tables. The controller calculates the feasible route and appropriate cycle parameters under the constraints of available spatial resources, temporal resources, and QoS requirements, and obtains the SID label stack corresponding to the path. (3) The control plane assigns the SIDs to the talker. Finally, CSQF-enabled network equipments reserve precise duration time for specified packets and forward them by parsing the topmost SID exhibited in the label stacks.

Theoretically, assuming that each output port contains two cyclic queues and the flow is successfully scheduled, a simple but general calculation method for the maximum delay D_{max} and the minimum delay D_{min} is:

$$D_{max} = \sum_{i=1}^h (LD_i + PD_i) + (h + 1)T, \quad (1)$$

$$D_{min} = \sum_{i=1}^h (LD_i + PD_i) + (h - 1)T, \quad (2)$$

$$J_{e2e} = D_{max} - D_{min} = 2T, \quad (3)$$

where LD is the link delay, PD is the process delay, h is the number of hops, and T is the cycle size. More importantly, since the packet can only fluctuate at the sending cycle of the first hop and the receiving cycle of the last hop, the end-to-end jitter J_{e2e} is strictly limited to $2T$ regardless of network hops.

Furthermore, the segment routing (SR) used by CSQF is also a source routing technique that can implement the explicit route. At the source node, all forwarding decisions towards the destination node have been carried in the SID labels. Hence, the intermediate and egress nodes do not need to maintain per-flow states. This characteristic enhances the scalability of CSQF, enabling it to schedule an extensive array of flows.

III. MOTIVATION

This section presents the methods to construct the CSQF model and compute the global cycle tags.

A. How to Model the CSQF?

CSQF only specifies an underlying packet scheduling mechanism on the data plane, which brings a significant problem of network-wide traffic planning to the control plane. To be more specific, how to construct the CSQF mathematical model and how to implement the SID calculation need to be solved. Next, We refer to the CQF in the range of local area to analyze the key points, i.e., link delays and cycle mapping relationships between adjacent nodes, in the process of modeling CSQF.

The features of local area include [13]: (1) The network diameter is restricted to a small scale, such as seven hops. (2) The time on switches can be strictly synchronized. (3) The propagation latency can be ignored. Based on these features, CQF supposes that the cycle length exceeds the summation of transmission latency, link latency, processing latency, and queuing latency. As detailed in Fig. 2(a), the CQF-enabled switch has two queues, and each queue's behavior is controlled by the receive (Rx) and transmit (Tx) gates. Determined by the gate control list (GCL), the two queues conduct enqueue and dequeue actions alternately. Thus, in a single cycle of T , the packet can be sent from the upstream device and received by the downstream device, then forwarded to the next-hop device in the subsequent cycle. As depicted in Fig. 2(b), if the packet

is the last issued and first arrived, the minimum latency is $(H - 1) \times T$, where H is the number of hops. In contrast, a packet takes the maximum delay of $(H + 1) \times T$ when it is the first sent and last received.

However, in wide-area networks, accurate time synchronization [20] is not easy to obtain and the varied propagation latency cannot be regarded as zero. Hence, it is not trivial to fix the per-hop latency to a certain cycle time T . To address these challenges, CSQF relaxes the synchronized time to the frequency [21], i.e., all switches maintain the same clock frequency but do not require the same initial phase, which introduces the initial phase deviation between devices. Then, CSQF enlarges the two queues of CQF to multiple queues, where one queue is for transmitting packets and the others for receiving packets. Fig. 2(c) depicts an instance of three-queues CSQF. Each queue corresponds to a cycle, and the queues dequeue packets in a periodic pattern. More than one receiving queues are utilized to absorb a certain amount of traffic bursts, but the mapping relationship between link delays and cyclic queuing behavior is still undefined.

Based on the above analysis, we propose the cycle tags planning (CTP), an integer programming model for the CSQF. First, we argue that switches can be aware of the initial phase deviation and update it to the controller. The cycle mapping pattern still holds if we consider the phase deviation is 0 [14]. Thus, for simplicity but without loss of generality, CTP assumes an initial phase deviation of 0 in the control plane as the basis of the scheduling model. Second, our CTP model decouples link delays from the cycle time T to hold a constant queue rotation duration. Specifically, the irregular link delay is divided by the cycle time and rounded up. Third, to unify the link delay and cyclic queuing behavior, we model the underlying network resources as time-discrete queue resource blocks. An auxiliary variable named arriving cycle is utilized to map the arriving time of packets to an appropriate receiving queue, which ensures aligned adjacent cycles. More details of CTP model are in Section IV.

B. How to Calculate the Cycle Tags?

Another key challenge for CSQF is how to compute the cycle tags for each flow under the CTP model. Since multiple flows will compete for the queue resources of each output port along the path, an efficient scheduling algorithm is needed to not only maximize the number of flows that meet the deadline, but also avoid breaking the maximum queue length constraints. In addition, for different network scenarios, how to set appropriate configuration parameters (such as the queue number and the cycle size) also needs to be investigated.

Specifically, there are two typical traffic access situations in real deployment scenarios: access-aware [17] [22], and access-unaware. Access-aware means that access network devices are gateways that can negotiate with terminal hosts and control when traffic will enter the CSQF-enabled network domain. Unawareness of the access indicates that the flow's arrival time of the first hop is uncontrollable. Thus, to make the cycle tags computation adapt to practical deployments, we propose two intuitive flow scheduling methods. One is to set the flow offset

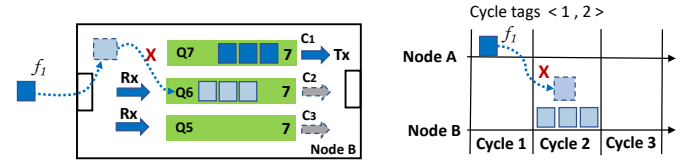


Fig. 3. An access-aware scenario with the queue length of three packets. The node A is the access gateway device of the CSQF-enabled network domain.

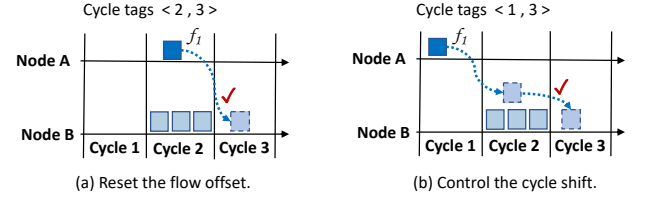


Fig. 4. An example of the flow offset and cycle shift (FO-CS) method. The flow offset operation decides the packet's arrival time at the first hop. The cycle shift optimizes the selection of receiving queues at each node.

at the first hop (i.e., access-aware), and the other is to control the cycle shift at each receiving queue (i.e., access-unaware).

To make it clear, we design a simple access-aware scenario where the maximum queue capacity is limited to three packets. As shown in Fig. 3, Node A functions as the access gateway device, and there's a time-sensitive flow (f_1) directed towards the downstream node, Node B. It is not allowed to enqueue the receiving queue Q_6 , because Q_6 is already at full capacity. One method, as demonstrated in Fig. 4(a), is to change the flow offset. By delaying the sending start time of flow f_1 at Node A by one cycle, the overflow at queue Q_6 can be circumvented. An alternative strategy involves adjusting the cycle shift, as seen in Fig. 4(b). Here, the flow f_1 is deferred to enqueue the queue Q_5 . Consequently, both methods ensure that the flow f_1 is successfully scheduled and transmitted out during Cycle 3. The difference is that the flow offset operation can search over the entire sending period time series, while the cycle shift operation is limited to available queue numbers. Note that Node A can execute both flow offset and cycle shift operations if it is access-aware, but can only execute the cycle shift operation if it is access-unaware. Moreover, if there is no available queue for choosing (e.g., all queues are full), the flow f_1 will fail to be scheduled. In this case, the flow needs to wait until some resources occupied by other flows are released, or the underlying network resources need to be expanded.

Inspired by the aforementioned exploration, our objective is to devise a heuristic flow scheduling algorithm called flow offset and cycle shift (FO-CS) that possesses the following characteristics:

Predictable performance: The algorithms should adhere to the constraints of bounded queue length and ensure time-sensitive flows reach their destination within the stipulated deadline and jitter.

High scalability: Our approach ought to exhibit high scalability, scheduling thousands of time-sensitive flows across long-distance industrial IoT networks.

Feasible execution time: Employing heuristic methods, our

and the transmitting queue, measured by cycle shift operations at the associated edge e_k . Typically, the Δ is an integer value that ranges from 0 to $N - 2$.

Fig. 6 presents an illustration of the CTP model from a comprehensive flow perspective. Flow f_1 initiates transmission at the first hop, specifically edge e_1 , during the flow offset of Cycle 0. Following a link latency equivalent to nearly two cycles, f_1 arrives at the edge e_2 in the Cycle 2. Then, it enqueues the second receiving queue, thus the value of $\Delta(f_1, e_2)$ is one cycle and f_1 will be transmitted at the edge e_2 in the Cycle 3. After that, it is received at the edge e_3 with $\Delta(f_1, e_3)$ of zero and transmitted in the Cycle 5. In its entirety, f_1 traverses through the path $\langle e_1, e_2, e_3 \rangle$ adhering to the designated cycle tags $\langle 0, 3, 5 \rangle$.

B. Integer Programming Inputs and Variables

Integer programming is a widely recognized mathematical method used to model network scheduling problems. The following are the inputs and decision variables.

1) Integer Programming Inputs:

- Physical topology graph $\mathcal{G} = \{\mathcal{V}, \mathcal{E}\}$.
- A collection of periodic time sensitive flows \mathcal{F} .
- Queue length L , queue number N , cycle size T_{cycle} .

2) Decision Variables:

- Flow offset, $\{\Omega_i \mid \Omega_i \in \Omega\}$.
- Cycle shift, $\{\Delta_{(f_i, e_k)} \mid f_i \in \mathcal{F}, e_k \in p_i\}$.

C. Core Constraints

1) *Hyper-cycle Constraint*: Various flows have different sending periods. A hyper-cycle is used to determine the time series bounds for the scheduling solution. As shown in (6), the hyper-cycle is defined as the least common multiple of all flows' sending periods (SP). Thus, the sending pattern repeats from the global perspective, and we only need to make the flow satisfy the scheduling constraints in one hyper-cycle. The hyper-cycle is a widely-used term in real-time system fields [13] [24]. In the same vein, this paper focuses on scheduling periodic TS flows, where the sending period is considered as an integer within a reasonable range to comply with industrial tasks. The sporadic flows can be delivered with other QoS methods, such as asynchronous traffic shaping and frame preemption. Moreover, in specific industrial scenarios, such as 5G TSCAI [25], IEC 60802 [26], and DetNet use cases [19], it is possible to register all types of devices and the periods of flows in advance. Consequently, the hyper-cycle can be established as the greatest value of the least common multiple derived from the flow periods of all known devices.

$$Hyper_cycle = LCM(SP). \quad (6)$$

2) *Cycle Constraint*: In this study, we define the granularity of scheduling by the cycle time. This mandates that every sending period must be divisible by the cycle time. Consequently, the upper bound of T_{cycle} aligns with the greatest common divisor of the sending periods of all flows, as depicted in (7). On the other hand, the lower bound of T_{cycle} must ensure that during its duration, all packets stored in a queue are

dispatched. This duration encompasses the cumulative value of the processing latency δ_p , maximum queuing latency δ_q , and transmission latency δ_m , as represented in (8).

$$\max(T_{cycle}) = GCD(SP). \quad (7)$$

$$\begin{aligned} \min(T_{cycle}) &= \lceil \delta_p + \max(\delta_q + \delta_m) \rceil \\ &= \lceil \delta_p + \frac{L \times MTU}{Bw} \rceil. \end{aligned} \quad (8)$$

In (8), Bw is the link capacity, MTU is the maximum transmission unit of packet size, and L is the maximum queue length. Typically, the value of T_{cycle} is chosen to be greater than its minimum, and $Hyper_cycle$ is divisible by T_{cycle} . Then, β is utilized to denote the total count of T_{cycle} in a $Hyper_cycle$ as presented in (9).

$$\beta = \frac{Hyper_cycle}{T_{cycle}}. \quad (9)$$

3) *Offset Constraint*: The offset of each flow determines the sending initial cycle at the first switch device (Ω_i) linked to the terminal node, which must be less than the defined sending period of the flow, as outlined in (10). In other words, the TS flow should be entirely forwarded within the current sending period to avoid stream interference that may occur during adjacent sending periods.

$$\forall i \in \{0, 1, 2, \dots, n-1\}, \quad 0 \leq \Omega_i < \frac{SP_i}{T_{cycle}}. \quad (10)$$

4) *Arriving Cycle Constraint*: As defined in (11), $A_{(f_i, e_k)}$ denotes the arriving cycle when the flow is arriving at the output port of a node. $t_{A_{(f_i, e_k)}}$ is the specific time point that packets may arrive. This constraint is satisfied by default if the cycle size is set to no less than the minimal value of T_{cycle} defined in (8).

$$\begin{aligned} \forall i \in \{0, 1, 2, \dots, n-1\}, \quad \forall e_k \in p_i, k \in \{1, 2, \dots, j\}, \\ A_{(f_i, e_k)} = \Omega_i + \sum_{h=0}^{k-1} \left\lceil \frac{LD_{(f_i, h)}}{T_{cycle}} \right\rceil + \sum_{h=0}^{k-1} \Delta_{(f_i, h)}, \\ A_{(f_i, e_k)} \times T_{cycle} \leq t_{A_{(f_i, e_k)}} \leq (A_{(f_i, e_k)} + 1) \times T_{cycle}. \end{aligned} \quad (11)$$

and $LD_{(f_i, 0)} = 0$, $\Delta_{(f_i, 0)} = 0$.

5) *Deadline Constraint*: For each flow, all packets need to reach their destination within the designated deadline, i.e.,

$$\begin{aligned} \forall i \in \{0, 1, 2, \dots, n-1\}, \\ 1 + \sum_{h=1}^j \left\lceil \frac{LD_{(f_i, h)}}{T_{cycle}} \right\rceil + \sum_{h=1}^j \Delta_{(f_i, h)} \leq \frac{D_i}{T_{cycle}}. \end{aligned} \quad (12)$$

6) *Flow and Edge-Cycle Mapping Constraint*: This constraint gives the mapping relationship between flow f_i and queue resource block $Q_{E(e_k)}^{T(t)}$ at the edge e_k and cycle t . If a flow f_i maps to a $Q_{E(e_k)}^{T(t)}$ successfully, i.e., the utilization of queue resource block does not exceed the queue length L , the value of the auxiliary variable $M(f_i, Q_{E(e_k)}^{T(t)})$ is 1, as depicted in (13). Otherwise, it is 0.

$$\begin{aligned}
& \forall i \in \{0, 1, 2, \dots, n-1\}, \\
& \forall e_k \in p_i, k \in \{1, 2, \dots, j\}, \forall t \in \{0, 1, \dots, \beta-1\}, \\
& M\left(f_i, Q_{E(e_k)}^{T(t)}\right) = 1. \\
& \text{s.t.} \\
& \lambda \in \left\{0, \dots, \frac{\text{Hyper}_{\text{cycle}}}{SP_i} - 1\right\}, \\
& t = \left(A_{(f_i, e_k)} + \Delta_{(f_i, e_k)} + \frac{\lambda \times SP_i}{T_{\text{cycle}}}\right) \% \beta.
\end{aligned} \tag{13}$$

The actual transmitting cycle at the edge is determined by the sum of the arriving cycle $A_{(f_i, e_k)}$ and the cycle shift $\Delta_{(f_i, e_k)}$. Given that a flow can be issued from its source multiple times within a $\text{Hyper}_{\text{cycle}}$, the variable λ specifies the sending period to which the flow pertains. Moreover, to ensure that the arriving time of flows does not exceed a $\text{Hyper}_{\text{cycle}}$, the transmitting cycle is subjected to a modulus operation with β . In summary, the variable of t encapsulates all the transmitting cycles a flow undergoes along its path within the range of a hyper-cycle.

7) *Bounded Queue Length Constraint*: As defined in (14), if a flow f_i is scheduled along the path successfully, i.e., for all the edges along the path the value $M\left(f_i, Q_{E(e_k)}^{T(t)}\right)$ is 1 while the deadline constraint and bounded queue length constraint are satisfied, then the value of S_i is 1. We call this kind of flow a schedulable flow. Otherwise, it is 0.

$$S_i = \begin{cases} 1, & \text{if } f_i \text{ is a schedulable flow} \\ 0, & \text{otherwise} \end{cases}. \tag{14}$$

The constraint on bounded queue length necessitates that the cumulative number of packets from all flows in any given queue not surpass the designated queue capacity, i.e.,

$$\begin{aligned}
& \forall i \in \{0, 1, 2, \dots, n-1\}, \\
& \forall e_k \in p_i, k \in \{1, 2, \dots, j\}, \forall t \in \{0, 1, \dots, \beta-1\}, \\
& \sum_{i=0}^{n-1} S_i \times M(f_i, Q_{E(e_k)}^{T(t)}) \times PK_i \leq L.
\end{aligned} \tag{15}$$

In this paper, the optimization objective is to maximize the number of schedulable TS flows, which is described as:

$$\text{CTP} : \max_{\Omega, \Delta} \sum_{i=0}^{n-1} S_i \tag{16}$$

$$\text{s.t.} \quad (6), (7), (8), (10), (12), (13), (14), (15)$$

where Ω is the variable of flow offsets ($\Omega = [\Omega_0, \dots, \Omega_{n-1}]^T$), and Δ is the variable of cycle shifts of flows ($\Delta = [\Delta_0, \dots, \Delta_{n-1}]^T$, $\Delta_i = [\Delta_{i,1}, \dots, \Delta_{i,j}]^T$).

D. Schedulability Analysis

In this paper, schedulability refers to the number of time-sensitive flows that could be scheduled by the network under constrained network resources and desired quality of service. Many factors such as traffic characteristics, flow sequence, and topology size, may affect scheduling capabilities. One

of the most important factors is the configurable parameter of queue length L . In (15), it seems that as L becomes larger, the number of packets each queue can hold increases, so the number of schedulable flows $\sum_{i=0}^{n-1} S_i$ improves (i.e., $\sum_{i=0}^{n-1} S_i \propto L$). Instead, we derive Theorem 1:

Theorem 1. *When the total network resources are constant (due to limited on-chip memory), the schedulability increases as the queue length L becomes smaller, i.e.,*

$$\sum_{i=0}^{n-1} S_i \propto \frac{1}{L}. \tag{17}$$

Proof. In (13), the total network resources are the number of resource blocks $Q_{E(e_k)}^{T(t)}$ with the cycle $T(t)$ and edge $E(e_k)$. For the flow mapping $M(f_i, Q_{E(e_k)}^{T(t)})$, the search space is $\prod_{i=0}^{n-1} \frac{SP_i}{T_{\text{cycle}}} \times (N-1)^n$, where n is the number of flows and N is the queue number. Thus, we have:

$$\sum_{i=0}^{n-1} S_i \propto \sum_{i=0}^{n-1} M(f_i, Q_{E(e_k)}^{T(t)}) \propto \frac{1}{T_{\text{cycle}}}. \tag{18}$$

In (8), there is:

$$T_{\text{cycle}} \geq \delta_p + \frac{L \times MTU}{Bw} \propto L. \tag{19}$$

Hence, derived from (18) and (19), there is $\sum_{i=0}^{n-1} S_i \propto \frac{1}{L}$. Theorem 1 is proved. \square

Corollary 1. *When the queue length L is set to the minimum value of 1, (13)-(15) can be relaxed to the well-investigated frame isolation constraints [24], in which the schedulability is maximized.*

Proof. When L takes the minimum value of 1, it means that each cycle $T(t)$ of each edge $E(e_k)$ can only store one packet. We assume that the packet number of each flow (i.e., PK_i) is no more than one. Then, the bounded queue length constraints in (13)-(15) will be relaxed as follows:

$$\begin{aligned}
& \forall f_i, f_j \in \mathcal{F}, e_k = (p_i \cap p_j) \in \mathcal{E}, i \neq j, \\
& \forall x \in \left\{0, \dots, \frac{\text{Hyper}_{\text{cycle}}}{SP_i} - 1\right\}, \\
& \forall y \in \left\{0, \dots, \frac{\text{Hyper}_{\text{cycle}}}{SP_j} - 1\right\}:
\end{aligned}$$

$$(A_{(f_i, e_k)} + \Delta_{(f_i, e_k)} + x \cdot \frac{SP_i}{T_{\text{cycle}}}) \geq A_{(f_j, e_k)} + \Delta_{(f_j, e_k)} + y \cdot \frac{SP_j}{T_{\text{cycle}}} \vee$$

$$(A_{(f_j, e_k)} + \Delta_{(f_j, e_k)} + y \cdot \frac{SP_j}{T_{\text{cycle}}}) \geq A_{(f_i, e_k)} + \Delta_{(f_i, e_k)} + x \cdot \frac{SP_i}{T_{\text{cycle}}} \tag{20}$$

Equation (20) indicates that for any two flows f_i and f_j in any sending period, there are two ways to avoid scheduling conflicts. The first is that the transmission time slot of flow f_i is after flow f_j , i.e., the left side of \vee . The second is that the transmission time slot of flow f_i is before flow f_j , i.e., the right side of \vee . Then, each flow independently occupies a cycle that can transmit an MTU-sized Ethernet frame. Since the packet size of flows (e.g., 100 Bytes) may be smaller than the MTU size, (20) still causes the waste of underlying time

slot resources. Further, we assume the specific transmission duration of a flow f_i is Θ_i and $t_{A(f_i, e_k)}$ is the specific time point that packet may arrive. (20) is converted to:

$$\begin{aligned} & \forall f_i, f_j \in \mathcal{F}, e_k = (p_i \cap p_j) \in \mathcal{E}, i \neq j, \\ & \forall x \in \left\{ 0, \dots, \frac{Hyper_{cycle}}{SP_i} - 1 \right\}, \\ & \forall y \in \left\{ 0, \dots, \frac{Hyper_{cycle}}{SP_j} - 1 \right\}: \\ & (t_{A(f_i, e_k)} + x \cdot SP_i \geq t_{A(f_j, e_k)} + \Theta_j + y \cdot SP_j) \vee \\ & (t_{A(f_j, e_k)} + y \cdot SP_j \geq t_{A(f_i, e_k)} + \Theta_i + x \cdot SP_i) \end{aligned} \quad (21)$$

Equation (21) is the frame isolation constraints [24], in which the discrete equal cycles are converted to continuous time resources. Each frame occupies a minimum time slot resource that is the same as its transmission duration. Hence, the scheduling capacity is maximized. \square

We adopt the bounded queue length constraints in (15) instead of frame isolation constraints in (21) for the following reasons. First, unlike LANs, it is hard to obtain fine-grained traffic characteristics (such as packet size or transmission duration) for all Industrial IoT flows in wide-area scheduling. Second, there is inevitable traffic aggregation in wide-area networks that causes queuing. Finally, the execution time of the solution grows exponentially as the queue length gets smaller. Thus, the queue length L should be set to an appropriate value to balance the schedulability and time costs.

V. ALGORITHM DESIGN

This section elaborates on the implementation of cycle tags computation, including the path selection, the basic flow scheduling, and the enhanced flow sequence algorithm.

A. Design Guidelines

The most naive method to calculate the SID information for TS flows is formulating multiple constraints and inputting the flows' parameters to the integer programming solver. However, this method is memory-intensive and may cost several hours to obtain a premium scheme for long-distance Industrial IoT scenarios. Fundamentally, the scheduling problem parallels the bin packing problem, which is NP-hard [14]. Hence, obtaining the optimal solution within a practical timeframe might be unattainable.

To reduce the complexity and improve the schedulability, we opt for computation-intensive heuristic methods to address this issue. Similar to the idea in [27], we split the CTP problem into a basic flow scheduling problem and an enhanced flow sequencing problem. In incremental online scheduling scenarios, the basic flow scheduling algorithm targets to quickly compute cycle tags for an ordered set of flows. For offline optimization contexts, the enhanced flow sequencing algorithm, which leverages the meta-heuristic Tabu search, focuses on establishing a complete order of the flow set to optimize the count of schedulable flows.

Algorithm 1: FO-CS Algorithm

Input: Flow set: \mathcal{F} , Edge-cycle resource: $Q_{E(e_k)}^{T(t)}$
Output: Scheduled flow set \mathcal{F}_{suc}

```

1 for  $f_i$  in  $\mathcal{F}$  do
2    $init \ \forall \ \Omega_i = 0, \Delta_i = 0;$ 
3    $Init\_result(f_i, Q_{E(e_k)}^{T(t)})$  according to (12)-(15);
4   if  $S(f_i) = 1$  then
5      $F_{suc} \leftarrow f_i;$ 
6     Break;
7   else
8     while  $\Omega_i < \frac{SP_i}{T_{cycle}}$  do
9       for  $e_k$  in  $p_i$  and  $M(f_i, Q_{E(e_k)}^{T(t)}) = 0$  do
10        while  $\Delta_{(f_i, e_k)} \leq N - 2$  do
11           $\Delta_{(f_i, e_k)} ++;$ 
12           $Compute(f_i, Q_{E(e_k)}^{T(t)})$  according
13            to (13); /* Cycle Shift
14            Part */
15          if  $M(f_i, Q_{E(e_k)}^{T(t)}) = 1$  then
16            Break;
17          if  $S(f_i) = 1$  then
18             $F_{suc} \leftarrow f_i;$ 
19            Break;
20          else
21             $\Omega_i ++;$  /* Flow Offset Part
22            */
23           $F_{fai} \leftarrow f_i;$ 
24 return  $\Omega_i, \Delta_i, \mathcal{F}_{suc};$ 

```

B. Path Selection

Generally, periodic TS flows account for a relatively small portion of bandwidth (e.g., 7% for scheduled flows in literature [6] and no more than 20% for critical control streams in literature [19]) compared to BE flows. For example, the differential protection traffic is just 64 kbps [4], but requires millisecond-level delay and microsecond-level jitter. Thus, to meet such stringent delay demands, the link delay weighs more than the bandwidth. In this study, we focus on CSQF scheduling and employ a weighted shortest path routing approach based on Dijkstra's algorithm. The link delay is denoted as the weight of each edge, and the path with the smallest end-to-end weight is selected as the routing path. The time complexity is $O(|V| \log |V| + |E|)$, where $|V|$ is the number of vertices and $|E|$ is the number of edges. Moreover, plenty of works have been done on the realization of routing for time-sensitive networks [9], such as Equal Cost Multi-Pathing (ECMP), Maximum Scheduled Traffic Load (MSTL), and segment routing. A load balancing based on CSQF is presented in [10], which can be applied to reduce the single point of congestion with additional complexity. Routing optimization with heuristic algorithms will be considered as future work.

C. Basic Flow Scheduling Algorithm

Based on the insights from Section III.C, our basic scheduling algorithm encompasses the cycle shift (CS), flow offset (FO), and a combined FO-CS algorithm. The FO-CS algorithm integrates elements from both the FO and CS. The FO algorithm operates under the premise that cycle shift operations in network output ports are zero, catering to situations where switches lack more than two queues. Simultaneously, the CS algorithm posits that TS traffic is dispatched with unpredictable initial times (offsets), addressing instances where the access arrival time point is uncontrolled.

The FO-CS algorithm sets both the offset value and cycle shift value to zero, sequencing the flows in a predetermined order, as outlined in Algorithm 1. For each flow f_i , the initial step determines whether $S(f_i)$ is 1 according to constraints (12)-(15). If $S(f_i)$ is 1, f_i will be put into F_{suc} (lines 1-6). Subsequently, if the flow is deemed unschedulable, the algorithm identifies the node where the mapping was unsuccessful. It then incrementally adjusts the cycle at that specific node, ensuring it stays within the constraints of the receiving queue's capacity (lines 9-13). Once a flow f_i is scheduled successfully along a route, it will be placed into the F_{suc} set (lines 14-16). Otherwise, the value of flow offset is increased by one and re-operates the cycle shift part considering the constraint of offset (lines 17-18). If the flow still cannot be scheduled after traversing all the flow offset and cycle shift operations, the flow will be placed into F_{fai} (line 19). Finally, the algorithm outputs scheduling parameters of Ω_i and Δ_i for each scheduled flow f_i in schedulable flow set F_{suc} . The CS part is preferentially executed because it has a smaller search space and lower time complexity than FO. Note that the worst-case time complexity of this FO-CS algorithm is $O(\sum_{i=0}^{n-1} \frac{SP_i}{T_{cycle}} \times N \times H)$, where n is the number of flows, N is the queue number at each output port, and H is the number of hops. The queue number N and the hop number H are bounded in a specific network. Therefore, the worst-case time complexity is $O(\sum_{i=0}^{n-1} \frac{SP_i}{T_{cycle}})$ for the FO-CS algorithm.

The FO-CS algorithm is flexible and efficient within the following three aspects. First, the maximum queue length and queue number can be adjusted with the increase of flow number and topology size. Second, the FO algorithm and CS algorithm can be utilized respectively under different scheduling scenarios, such as symmetric and asymmetric topologies. In symmetric topologies, traffic aggregation can be greatly alleviated by first-hop shaping of access switches; thus the flow offset algorithm works well independently and reduces the computational overhead. Third, the FO-CS algorithm quickly generates incremental flow scheduling solutions, which supports online long-distance Industrial IoT traffic transmission.

D. Enhanced Flow Sequence Algorithm

The enhanced flow sequence algorithm creates a varied scheduling order for the flow set F , to maximize the resulting number of schedulable time-sensitive flows computed by the FO-CS algorithm. The maximum number of the search space for the sequencing problem is $n!$, where n is the number of flows. Since the brute force approach cannot be scaled to large

Algorithm 2: Tabu FO-CS Algorithm

Input: Flow set: \mathcal{F} , Edge-cycle resource: $Q_{E(e_k)}^{T(t)}$

Output: Scheduled flow set \mathcal{F}_{suc}

```

1  $curr\_result \leftarrow Init\_result(\mathcal{F}, Q_{E(e_k)}^{T(t)})$ ;
2  $best\_order \leftarrow Curr\_order(curr\_result)$ ;
3  $best\_result \leftarrow curr\_result$ ;
4 while Termination criteria not satisfied do
5    $curr\_order \leftarrow Neighbor(curr\_order)$ ;
6    $curr\_result \leftarrow Gen\_best(curr\_order)$ ;
7   if  $curr\_result$  better than  $best\_result$  then
8      $best\_order \leftarrow curr\_order$ ;
9      $best\_result \leftarrow curr\_result$ ;
10 return  $best\_order, best\_result, F\_suc$ ;

```

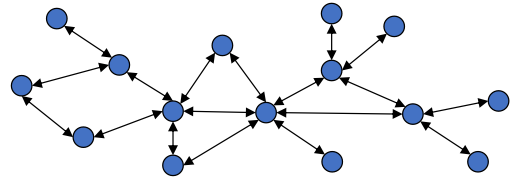
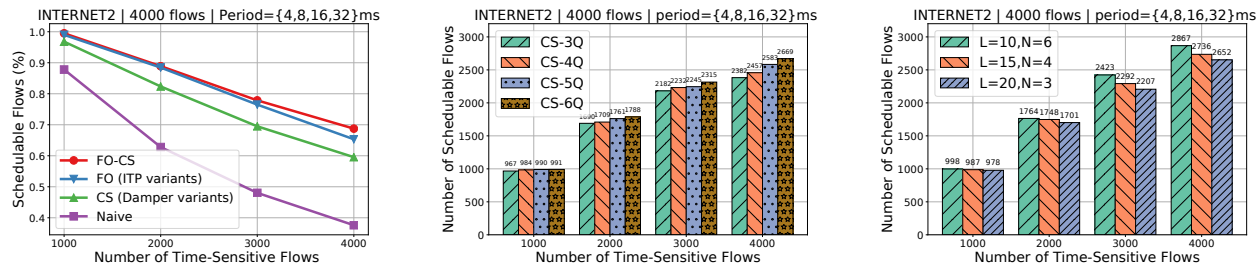


Fig. 7. ER topology: an example of graph $G(15, 18)$.

problem sizes, it is unacceptable in real-world applications. There are many meta-heuristic algorithms to approximate the optimal solution. Due to the advantage of recording the previously searched solutions, we utilize the Tabu search [27] with a simplified Tabu list as a guided exploration of the solution space. Wide-area deployment often is incapable of knowing all traffic prior. Thus, feasible online solutions are more appropriate than optimal offline solutions. We leave other meta-heuristic offline searching strategy with domain-specific knowledge (DSK) as future work.

As outlined in Algorithm 2, the Tabu FO-CS algorithm generates the initial results using a random order, and defines it as the current result (lines 1-3). Then, the neighborhood of the current order is derived from the exchanging mode [13]. In this mode, a subset of mapped flows in F_{suc} are randomly removed by cleaning the queue resource block associated with these flows. Following this, the flows in F_{fai} are integrated into F_{suc} until no enough network resources can be allocated (lines 5-6). Exchange operations are recorded in (and removed from) the Tabu list to avoid local optima. If the current result is better than the previous best result, it will be marked as the best result and selected as the next solution for the next iteration. To reduce the superfluous search, the termination criteria are set based on two conditions: either the number of iterations surpasses the maximum threshold K , or there is no improvement observed in the best result over the past P iterations (line 4). The efficacy of the Tabu FO-CS algorithm can be adjusted by varying the values of K and P . While setting larger values for both parameters might lead to superior outcomes, it could significantly prolong the computation time.



(a) Naive vs Flow offset and cycle shift (FO-CS). (b) Effect of queue number on cycle shift (CS). (c) Effect of memory allocation on FO-CS.

Fig. 8. Simulation results for the influence of FO-CS algorithms on the number of schedulable flows.

VI. EVALUATIONS

This section presents the simulation results of FO-CS and Tabu FO-CS algorithms. Firstly, we outline the simulation setup. Then, we analyze the algorithm performance, including the number of schedulable flows, time costs, and scalability.

A. Simulation Setup

All evaluations are conducted on a computing device powered by four Intel i5-8259U CPUs, operating at a base clock speed of 2.3 GHz, and complemented with 16 GB of RAM.

1) *Topology Selection*: The INTERNET2 [28] stands as a pivotal advanced network where research and trials of emerging technologies are conducted. These innovations are then integrated into the next iteration of the Internet, including technologies like IPv6, MPLS, and QoS. Industrial control from remote locations frequently encompasses long-distance transmissions across various regions. To assess the efficacy of our proposed mechanism, we select a segment from the advanced Layer 3 service of INTERNET2's backbone in 2016 as a test topology [28]. This segment comprises eight nodes situated in cities including Atlanta, Chicago, Cleveland, Ashburn, Washington, and New York. The geographical distance between these nodes serves as a proxy for the link length. The link delay is computed by dividing the link length by two-thirds the speed of light. To verify the effect of the link connectivity, we leverage the Erdős-Rényi (ER) model to build a directed weighted random graph with fifteen vertices. An instance of the $G_{(n,m)}$ random topology is depicted in Fig. 7, where n indicates the number of nodes and m indicates the number of edges [9] [16]. The link delay is randomly selected from 0.1 ms to 2 ms.

2) *Resource Configuration*: In our experiments, we configure resources based on parameters such as link bandwidth, queue length, T_{cycle} size, and queue count. Specifically, we allocate a reserved link bandwidth of 1 Gbps, establish each CSQF queue's length at 10, and define the T_{cycle} size as 125 μ s. If the time-sensitive packets do not require a relatively low deadline and the on-chip memory is surplus, the queue length can be set larger. The T_{cycle} size is set to 125 μ s for three reasons. First, the transmission delay for 10 MTU-sized packets is about 120 μ s according to the (8). Second, the minimum value of T_{cycle} is selected to increase the search space of the cycle time. Third, the T_{cycle} better be a divisor

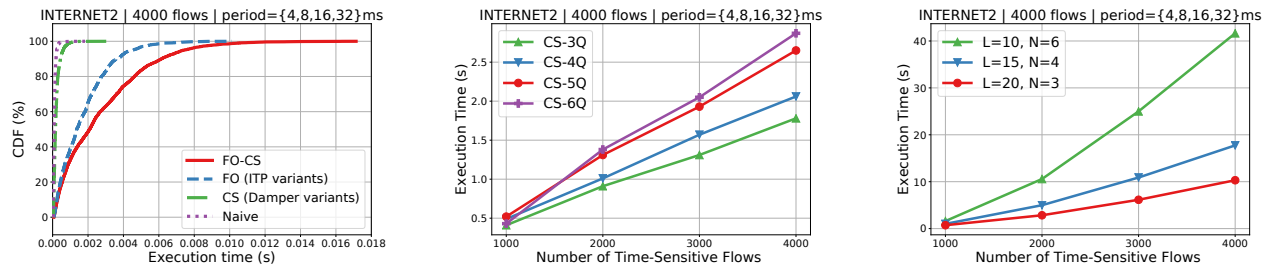
of $Hyper_{cycle}$ to simplify the calculation. For TS traffic, the queue count N is set to vary between 2 and 6. When N equals 2, it implies that additional cycle shifts cannot be accommodated.

3) *Traffic Characteristics*: For each flow f , its source and destination are determined by randomly selecting two distinct nodes with a uniform probability. Flows are created in alignment with the traffic patterns observed in wide area control and monitoring systems (as outlined in the IEC 61850) and the industrial machine-to-machine context of the DetNet use case [26] [19] [29]. Typically, the sending period of every flow is in the range of milliseconds, we emulate it by stochastically selecting one item from the assembly of {4, 8, 16, 32} ms. The number of packets in each period for a given flow is chosen from the assembly of {1, 2, 3}. The deadline of flows ranges from 30 ms to 50 ms.

B. Simulation Results for FO-CS

1) *Impact on the Schedulability*: The schedulability is indicated by the number of schedulable flows. Under the condition of Internet2 topology, we partition the flow counts into four groups from 1000 to 4000, and each group is executed five times to count average scheduled flows. The default queue number is set to 3.

Firstly, we juxtapose the performance of FO-CS algorithm with that of FO, CS, and naive algorithms, considering varying flow counts as presented in Fig. 8(a). Specifically, the naive algorithm dispatches packets as they're produced, without regulating the cycle shift or sending time. To compare the performances of CSQF with other mechanisms, the FO algorithm with two queues, which decides the packet's arrival cycle offset at the first hop, can be considered a benchmark of the ITP [13]. Damper [30] defers packets for a specified amount of time hop by hop. The CS algorithm with more than two queues, which optimizes the selection of receiving queues at each node, can be considered a variant of the Damper. As we scale up the flow number, the advantages of FO-CS become more pronounced compared to the naive approach. The maximum improvement observed is a commendable 31.2% over the naive approach and 9.2% over the CS under dealing with 4000 flows. Fig. 8(a) further indicates that FO's scheduling capability is nearly on par with FO-CS. This is because the flow offset operation offers a broader search space than



(a) Naive vs Flow offset and cycle shift (FO-CS). (b) Effect of queue number on cycle shift (CS). (c) Effect of memory allocation on FO-CS.

Fig. 9. Simulation results for the influence of FO-CS algorithms on the execution time.

the cycle shift, making offset control more impactful than managing the cycle shift at every hop. For individual flow scheduling in high-volume traffic scenarios, FO-CS remains valuable, offering the benefit of incremental cycle adjustments at each hop.

In situations where the flow offset is unmanageable at the access node, the CS algorithm can operate independently with varying queue numbers. Fig. 8(b) examines the distinctions among the CS-3Q, CS-4Q, CS-5Q, and CS-6Q algorithms. The CS-6Q algorithm consistently outperforms the others across all flow levels. The performance disparity between CS-6Q and CS-3Q fluctuates between 2.4% and 7.18%. Notably, as flow numbers rise, the effectiveness of the CS algorithm improves more markedly with a large queue number.

Since the on-chip memory is limited, Fig. 8(c) evaluates the effect of memory allocation for FO-CS algorithm. Assuming the buffer is sixty packets at each output port, we divide the buffer into three solutions: $L=10$ and $N=6$, $L=15$ and $N=4$, $L=20$ and $N=3$. Evaluation results show that the queue length of 10 has better schedulability than the other two. The maximal improvement is 7.2% compared to the queue length of 20 when the flow number is 3000. Thus, fine-grained queue division can improve the scheduling capability.

2) *Impact on the Execution Time*: The algorithm execution time is independent of the flows' sending period. Before sending packets, the talker sends requests to the controller, ensuring that time slot resources are strictly reserved in all sending periods. Thus, the algorithm just needs to be executed once when a flow is initially considered to be accommodated. Fig. 9(a) depicts the cumulative distribution function (CDF) of per-flow execution time for FO-CS, FO, CS, and naive algorithms. For the FO-CS approach, each flow's execution time does not exceed 18 milliseconds, 90% of per-flow execution times are under 6 milliseconds, and the total time for 4000 flows is about 20 seconds, revealing that all our algorithms have a feasible time for execution. The CS curve is on top of the FO and the FO-CS, suggesting that managing the per-flow offset operation is more time-consuming than adjusting the per-node cycle shift. Fig. 9(b) shows the total execution time of the CS algorithm when scheduling 1000, 2000, 3000, and 4000 flows respectively. The total execution time of CS algorithms with different queue numbers varies from 0.41 seconds to 2.87 seconds. The cycle shift with a larger queue number will slightly increase the running time.

Fig. 9(c) shows the total running time of the FO-CS algorithm with different flow number groups and memory allocation solutions. When scheduling 1000 flows, the execution time for all solutions maintains at the same low level. However, the execution time of the first solution ($L=10$ and $N=6$) increases sharply when the flow number increases. At the flow level of 4000, the execution time of the first solution is twice that of the second solution and four times that of the third solution. Consequently, the queue division is not as fine as possible when considering the execution time overhead.

C. Simulation Results for Tabu FO-CS

Furthermore, we evaluate the performance of Tabu FO-CS under different topologies, including the linear, the ring, and a part of Internet2. For the termination criteria in Algorithm 2, we set the maximum iterations K to 1000 and the maximum repetitions P to 100. The queue length of 10 and queue number of 4 are adopted for the FO-CS algorithm based on the previous evaluations. Each test is performed five times, and we calculate the average number of schedulable flows and the mean time consumed.

1) *Impact on the Schedulability*: In Fig. 10(a), we juxtapose the performance of the Tabu FO-CS algorithm against the FO-CS and naive algorithms. The evaluations show that the Tabu FO-CS algorithm can schedule 94.45% of flows at the level of 2000 flows under the topology of Internet2. In all topologies, the Tabu FO-CS algorithm consistently outperforms the FO-CS algorithm in scheduling outcomes. The maximal improvement is 7.9% compared to FO-CS under the ring topology, and 31.65% compared to the naive algorithm under the topology of Internet2.

2) *Impact on the Execution Time*: Fig. 10(b) illustrates the execution time of the above algorithms. We take the logarithmic function of \log_{10} for the execution time as its value varies widely. The evaluations exhibit that the execution time of the Tabu FO-CS algorithm is on the order of ten thousand seconds, while the FO-CS algorithm is on the order of ten seconds. Thus, the Tabu FO-CS algorithm is suitable for offline optimization scenarios, and the FO-CS algorithm can be applied to the rapid generation of a scheduling solution.

3) *Effect of the Link Connectivity*: Another key performance of the algorithm is scalability. The number of links in the network will have a certain impact on the number of

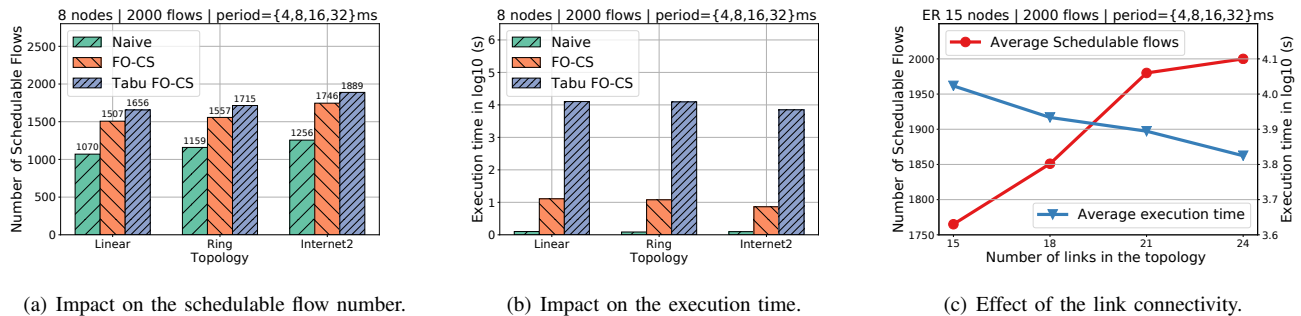


Fig. 10. Simulation results for the Tabu FO-CS algorithms under different topologies.

schedulable flows and algorithm execution time. As depicted in Fig. 10(c), in the case of 15 links, the Tabu FO-CS algorithm successfully schedules 88.25% of the flows with an average time cost of 2.9 hours. In the case of 24 links, the number of schedulable flows improves by 11.75% with a reduction of 36.68% in the average execution time. The reason is that increased links provide more time slot resources and reduce the possibility of scheduling failures.

VII. RELATED WORKS

There are plenty of related works about small-scale deterministic flow transmission in local Industrial IoT systems, but few works on that in large-scale Industrial Internet. Next, we mainly present related works around the CSQF-based time-sensitive scheduling mechanism.

Small-scale Time-sensitive Networks: In automotive, aerospace, and Industrial IoT scenarios, the enhanced real-time Ethernet technologies, such as the Time-Triggered Ethernet and TSN, are replacing the traditional fieldbus. Based on global time synchronization, TTE requires strict planning of the sending start time of each packet. The authors in [31] studied the synthesis of scheduling time tables in TTE with SMT/OMT solver. Furthermore, TSN provides a series of time-based gate-controlled mechanisms to guarantee bounded-delay transmission. The majority of research on TSN centers around the creation and refinement of gate control lists [16] [32] [33]. Recently, Yan *et al.* [13] proposed planning methods to map the flows onto the ping-pong queue resources of CQF.

Long-distance Industrial IoT Networks: CQF is extended to the CSQF to enable the multi-queues scheduling by the IETF DetNet working group. The study [34] examined the CQF and Paternoster mechanisms within a standard industrial control loop, taking into account different link delays. The authors of [35] proposed a C-TSDN architecture, in which the CQF and CSQF protocols are jointly designed to realize seamless scheduling for factory IoT infrastructure. [17] managed to provide layer-3 time-sensitive transmission down to the field level, which achieves remote industrial control in a heterogeneous network. Moreover, Large-scale Deterministic Network (LDN) [36] classifies cycle mapping into swap mode and stack mode, and emphasizes the ingress shaping function [22]. CSQF can be considered as the stack-mode-based LDN. The authors of [14] addressed the joint routing and scheduling

issues for CSQF. They target to the path generation with feasible arc-cycle capacity, which cannot adaptively adjust the cycle tags. We solve the cycle tag computation problem, especially considering the long-distance link delay and adjacent cycle mapping relationship. To our knowledge, this is the pioneering study introducing the global cycle tag planning for the CSQF.

VIII. CONCLUSION

This study introduced the CTP, a comprehensive integer programming framework tailored for CSQF-driven network-wide TS flow scheduling, which can make CSQF practical for long-distance Industrial IoT scenarios. The model decouples link delays from the cycle time, ensuring uniform queue rotation durations and addressing varying link delays by mapping the arriving cycle to a specific receiving queue. To avoid queue overflows under traffic aggregations, we devised the heuristic FO-CS algorithm for efficient cycle tag calculation. Empirical evaluations underscored the efficacy of FO-CS, marking a notable 31.2% enhancement in the number of schedulable flows compared to the Naive method. The Tabu FO-CS algorithm approaches 94.45% in scheduling 2000 flows. In the future, we will optimize multiple objectives and leverage deep reinforcement learning to solve the model.

REFERENCES

- [1] S. Vitturi, C. Zunino, and T. Sauter, "Industrial communication systems and their future challenges: next-generation Ethernet, IIoT, and 5G," *Proceedings of the IEEE*, vol. 107, no. 6, pp. 944–961, 2019.
- [2] M. Ulbricht, S. Senk, H. K. Nazari, H.-H. Liu, M. Reisslein, G. T. Nguyen, and F. H. P. Fitzek, "Tsn-flextest: Flexible tsn measurement testbed," *IEEE Transactions on Network and Service Management*, 2023.
- [3] I. Pelle, F. Paolucci, B. Sonkoly, and F. Cugini, "Latency-sensitive edge/cloud serverless dynamic deployment over telemetry-based packet-optical network," *IEEE Journal on Selected Areas in Communications*, vol. 39, no. 9, pp. 2849–2863, 2021.
- [4] B. Hu and H. Gharavi, "A hybrid wired/wireless deterministic network for smart grid," *IEEE Wireless Communications*, vol. 28, no. 3, pp. 138–143, 2021.
- [5] M. Groshev, C. Guimarães, J. Martín-Pérez, and A. de la Oliva, "Toward intelligent cyber-physical systems: digital twin meets artificial intelligence," *IEEE Communications Magazine*, vol. 59, no. 8, pp. 14–20, 2021.
- [6] A. Nasrallah, A. S. Thyagaturu, Z. Alharbi, C. Wang, X. Shao, M. Reisslein, and H. ElBakoury, "Ultra-low latency (ULL) networks: the IEEE TSN and IETF DetNet standards and related 5G ULL research," *IEEE Communications Surveys Tutorials*, vol. 21, no. 1, pp. 88–145, 2019.

- [7] L. Zhao, P. Pop, and S. Steinhorst, "Quantitative performance comparison of various traffic shapers in time-sensitive networking," *IEEE Transactions on Network and Service Management*, vol. 19, no. 3, pp. 2899–2928, 2022.
- [8] ITU-R, *IMT traffic estimates for the years 2020 to 2030*, 2015, https://www.itu.int/dms_pub/itu-r/opb/rep/R-REP-M.2370-2015-PDF-E.pdf.
- [9] N. G. Nayak, F. Dürr, and K. Rothermel, "Incremental flow scheduling and routing in time-sensitive software-defined networks," *IEEE Transactions on Industrial Informatics*, vol. 14, no. 5, pp. 2066–2075, 2017.
- [10] S. Chen, J. Leguay, S. Martin, and P. Medagliani, "Load balancing for deterministic networks," in *Proc. 2020 IFIP Networking*, 2020, pp. 785–790.
- [11] Y. Huang, S. Wang, S. Zhu *et al.*, "Programmable cycle-specified queue for deterministic networking," in *Proceedings of the ACM SIGCOMM Conference*, 2023, pp. 1132–1134.
- [12] S. Wang, B. Wu, C. Zhang, Y. Huang, T. Huang, and Y. Liu, "Large-scale deterministic IP networks on CENI," in *Proc. IEEE INFOCOM WKSHPS*, 2021, pp. 1–6.
- [13] J. Yan, W. Quan, X. Jiang, and Z. Sun, "Injection time planning: making CQF practical in time-sensitive networking," in *Proc. IEEE INFOCOM*, 2020, pp. 616–625.
- [14] J. Krolkowski, S. Martin, P. Medagliani, J. Leguay, S. Chen, X. Chang, and X. Geng, "Joint routing and scheduling for large-scale deterministic ip networks," *Computer Communications*, vol. 165, pp. 33–42, 2021.
- [15] Y. Huang, S. Wang, X. Zhang, T. Huang, and Y. Liu, "Flexible cyclic queuing and forwarding for time-sensitive software-defined networks," *IEEE Transactions on Network and Service Management*, vol. 20, no. 1, pp. 533–546, 2023.
- [16] J. Falk, F. Dürr, and K. Rothermel, "Exploring practical limitations of joint routing and scheduling for TSN with ILP," in *Proc. IEEE Embedded and Real-Time Computing Systems and Applications*, 2018, pp. 136–146.
- [17] A. Badar, D. Z. Lou, U. Graf, C. Barth, and C. Stich, "Intelligent edge control with deterministic-IP based industrial communication in process automation," in *Proc. Network and Service Management*, 2019, pp. 1–7.
- [18] *3GPP TS22261 v16.2.0. Service requirements for the 5G system*, 2017, https://www.3gpp.org/ftp/Specs/archive/22_series/22.261/22261-g20.zip.
- [19] *IETF deterministic networking use cases*. [Online]. Available: <https://datatracker.ietf.org/doc/rfc8578/>.
- [20] "IEEE standard for local and metropolitan area networks - timing and synchronization for time-sensitive applications in bridged local area networks," *IEEE Std 802.1AS-2011*, pp. 1–292, 2011.
- [21] J.-L. Ferrant, M. Gilson, S. Jobert, M. Mayer, M. Ouellette, L. Montini, S. Rodrigues, and S. Ruffini, "Synchronous Ethernet: a method to transport synchronization," *IEEE Communications Magazine*, vol. 46, no. 9, pp. 126–134, 2008.
- [22] B. Liu, S. Ren, C. Wang *et al.*, "Towards large-scale deterministic IP networks," in *IFIP Networking Conference*, 2021, pp. 1–9.
- [23] Y. Huang, S. Wang, T. Feng, J. Wang, T. Huang, R. Huo, and Y. Liu, "Towards network-wide scheduling for cyclic traffic in IP-based deterministic networks," in *2021 4th International Conference on Hot Information-Centric Networking (HotICN)*, 2021.
- [24] M. Vlk, Z. Hanzálek, K. Brejchová, S. Tang, S. Bhattacharjee, and S. Fu, "Enhancing schedulability and throughput of time-triggered traffic in ieee 802.1qbv time-sensitive networks," *IEEE Transactions on Communications*, vol. 68, no. 11, pp. 7023–7038, 2020.
- [25] A. Larrañaga, M. C. Lucas-Estañ, I. Martínez, I. Val, and J. Gozalvez, "Analysis of 5g-tsn integration to support industry 4.0," in *IEEE ETFA*, 2020, pp. 1111–1114.
- [26] IEC 60802 Standard. [Online]. Available: <http://grouper.ieee.org/groups/802/1/files/public/docs2019/60802-Hotta-Traffic-Types-Mapping-to-TSN-Mechanism-0119-v01>.
- [27] R. Macchiaroli, S. Mole, and S. Riemma, "Modelling and optimization of industrial manufacturing processes subject to no-wait constraints," *International Journal of Production Research*, vol. 37, no. 11, pp. 2585–2607, 1999.
- [28] J. Castillo-Velazquez, D. Serrano-Martinez, and A. Morales, "Emulation of the connectivity of backbone and management for the layer 3 service of internet2: 2016 Topology," in *Proc. IEEE Central America and Panama Convention*, 2017, pp. 1–4.
- [29] D. Paul, A. Astrit, and P. David, "Time sensitive networks for flexible manufacturing testbed - description of converged traffic types." [Online]. Available: <https://hub.iiconsortium.org/tsn-converged-traffic-types>.
- [30] E. Mohammadpour and J.-Y. Le Boudec, "Analysis of dampers in time-sensitive networks with non-ideal clocks," *IEEE/ACM Transactions on Networking*, vol. 30, no. 4, pp. 1780–1794, 2022.
- [31] W. Steiner, "An evaluation of SMT-based schedule synthesis for time-triggered multi-hop networks," in *Proc. Real Time Syst. Symp.*, 2010, pp. 375–384.
- [32] Z. Feng, M. Cai, and Q. Deng, "An efficient pro-active fault-tolerance scheduling of ieee 802.1qbv time-sensitive network," *IEEE Internet of Things Journal*, vol. 9, no. 16, pp. 14501–14510, 2022.
- [33] G. Miranda, E. Municio, J. Haxhibeqiri, J. Hoebeke, I. Moerman, and J. M. Marquez-Barja, "Enabling time-sensitive network management over multi-domain wired/wi-fi networks," *IEEE Transactions on Network and Service Management*, vol. 20, no. 3, pp. 2386–2399, 2023.
- [34] A. Nasrallah, V. Balasubramanian, A. S. Thyagaturu, M. Reisslein, and H. Elbakoury, "Large scale deterministic networking: a simulation evaluation," *ArXiv*, vol. abs/1910.00162, 2019.
- [35] Y. Huang, S. Wang, T. Huang, and Y. Liu, "Cycle-based time-sensitive and deterministic networks: Architecture, challenges, and open issues," *IEEE Communications Magazine*, vol. 60, no. 6, pp. 81–87, 2022.
- [36] Q. li, X. Geng, B. Liu, T. Eckert, L. Geng, and G. Li, *Large-Scale Deterministic IP Network*, 2019, <https://datatracker.ietf.org/doc/html/draft-qiang-detnet-large-scale-detnet-05>.